JOURNAL OF MATERIALS SCIENCE 32 (1997) 1029–1038

Characterization of hypervelocity impact craters on chemical vapour-deposited diamond and diamond-like carbon films

R. RAMESHAM, S. BEST, M. F. ROSE, M. CRUMPLER
Space Power Institute, 231 Leach Science Center, Auburn University, Auburn, AL 36849, USA

Microwave plasma chemical vapour-deposited (CVD) process has been used to grow polycrystalline diamond films over silicon substrates. Diamond-like carbon (DLC) thin films were grown over silicon substrates using a microwave plasma disc reactor. Reactant gases of CH_4 and H_2 were used in both CVD processes. Some preliminary feasibility tests were performed on the possible applicability of diamond and diamond-like carbon thin films for space-protective applications against artificially simulated electrically actuated plasma drag hypervelocity impact of olivine particles. As-deposited films were analysed by Raman for their chemical nature. The morphology and dimensions of hypervelocity impact craters in diamond and DLC films was also studied by scanning electron microscopy (SEM) and optical microscopy. The velocity of debris particles was determined by high-speed photography using a streak camera. The size of the impact particles was determined by measuring the size of the holes formed in the mylar sheet mounted just above the target diamond and DLC film/silicon and coordinates of the impact sites were determined using the same apparatus.

1. Introduction

Diamond and diamond-like carbon films are remarkable materials for innumerable applications because of their unusual combination of physical and chemical properties [1–3]. Therefore, several potential applications can be anticipated in electronics, optics, and protective mechanical and thermal coatings. Surface coatings are important for space and commercial applications, in particular on thermal control schemes. The combined effects of micrometeoroids, atomic oxygen, solar radiation, and ionized particles, will degrade the properties of the coatings well before the substrate structure has outlived its usefulness. Consequently, there is a need for the development of advanced survivable materials coatings to extend the useful life of space components.

There are two types of particulate matter in space. One is the natural micrometeoroid environmental component. The second is a man-made component that prevails in certain mass regimes due to the constant injection of materials via innumerable launches. Man-made contributions range from fuel residue to a variety of derelict satellites weighing many kilograms. The probability of damage, caused by the micrometeoroid particles, increases as the spacecraft size increases. Therefore, it is appropriate at this stage to develop transparent, non-reflective surface coatings to protect various external surfaces of the spacecraft from impact damage by micrometeoroid and debris particles. All the coatings should be mechanically adherent and should be resistant to hypervelocity impact events. The maximum upper limit to the velocity distribution by natural micrometeoroid component and man-made component is of the order of 40 and 14–16 $km\,s^{-1}$, respectively. The long duration exposure facility (LDEF) has shown that the size of the space debris particles is in the range of 10^{-6}–10^{-3} g. These debris particles would generally have a significant erosion effect on metallic and dielectric coatings on various parts of the spacecraft. On impact, copious amounts of ejecta are evolved from the spacecraft in the impact zone. Therefore, the local micrometeoroid and debris environment are enhanced further by impact ejecta.

Micrometeoroid and space debris impacts are potential initiators of electrical breakdown in spacecraft systems where electrically biased surfaces are exposed to the space environment. Hypervelocity microparticles, which generate a plasma plume, can trigger electrical breakdown under the influence of an applied electric field, particularly at Low Earth Orbital (LEO) altitude. Hypervelocity micro-particles impact on spacecraft and space structures in LEO at velocities in the range of 7–20 $km\,s^{-1}$. The kinetic energy of the particle is converted to shock waves in the target material. As a result of impact copious amounts of ejecta and hot plasma are produced. These physical phenomena are known to be extremely damaging to low voltage spacecraft systems. The introduction of such phenomena in high voltage systems will initiate catastrophic electrical breakdown, intense arcing, and surface tracking of materials by virtue of the liberation of energetic neutral particles, ions, electrons, solid and liquid ejecta. Gehring and Warnica [4] have measured

0022–2461

the intensity of the flash produced by hypervelocity impacts in several experiments. Shaw *et al.* [5] have recently reported no conclusive results on hypervelocity impact tests on diamond films using a 2 MV Van de Graaff particle accelerator. The inconclusive results were due to the roughness of the diamond samples used and also due to hypervelocity impact limitations. The largest crater size observed on aluminium was 1.7 μm. They were not able to identify any crater on diamond because the surface roughness of diamond film dominated all surface features. The Space Power Institute of Auburn University has an in-house facility to study impact phenomena on spacecraft materials. In this paper, we provide results on characterization of impact craters in chemical vapour-deposited (CVD) diamond and diamond-like carbon (DLC) coated silicon substrates.

2. Experimental procedure

2.1. Diamond growth process

A microwave plasma (2.45 GHz) assisted CVD system (ASTeX, Woburn, MA) has been used to grow diamond films on scratched (0.25 μm diamond paste) silicon substrates. A schematic diagram of the diamond deposition system has been described earlier [6, 7]. The substrate was placed at the centre of the stage that was then loaded into the quartz bell-jar reactor. The reactor was evacuated to a base pressure of 10^{-4} torr (1 torr = 133.322 Pa). Plasma was obtained by adjusting pressure in the chamber, hydrogen flow rate, microwave power, and wave-guide tuning. The substrate was *in situ* heated by the microwave plasma to attain the desired substrate temperature and initiated the growth of diamond. UHP grade hydrogen and research grade CH_4 were used in our experiments. The temperature was monitored remotely by an optical pyrometer. Diamond deposition was started by injecting CH_4 into the system when the substrate reached a desired temperature. Diamond was grown on silicon substrate (area ≈ 1 in^2; ~ 6.45 cm^2). In total, four samples were prepared and mounted on the Al/Cu plate with a wax that could easily be removed by soaking in acetone. The effective area of diamond on silicon was 4^2 in (~ 25.8 cm^2) in an impact test. Typical deposition conditions to grow diamond were as follows: pressure 37.6 torr; forward power 802 W; reflected power 8 W; hydrogen flow rate 500 standard cm^{-3}; CH_4 flow rate 3.6 standard cm^3; substrate temperature 914°C; and deposition time 13–30 h. The deposition rate under these conditions was ~ 1 μm h^{-1}. A continuous film of diamond was usually obtained after 10–12 h growth.

2.2. Diamond-like carbon growth process

Diamond-like carbon thin films were grown over chemically cleaned 3 in. (~ 7.62 cm) diameter silicon substrates using microwave plasma (Power supply 2.45 GHz, 1.5 kW, ASTeX, Woburn, MA) disc reactor in the down-stream mode. The substrate temperature was approximately about 50 ± 10 °C. The substrate temperature was measured by laying the substrate over a J-type thermocouple. This DLC reactor was designed by Professor J. Asmussen's group at Michigan State University. A schematic diagram of the reactor is shown in Fig. 1 [8]. Typical deposition parameters employed to deposit adherent diamond-like carbon thin films were as follows: methane flow rate 5 standard cm^3 min; hydrogen flow rate 20 standard cm^3 min; forward power 200 W; reflected power < 10 W; down-stream mode; growth rate 0.66 μm h^{-1}. Very good quality smooth adherent thin films were formed over 3 in. (~ 7.62 cm) diameter silicon substrate.

2.3. Hypervelocity impact test

There are several approaches by which to investigate meteoroid and debris impact phenomena: (a) placing the desired materials in space for long duration, (b) use light gas gun technology to accelerate macro-projectiles for impact studies, and (c) employ plasma drag accelerators to drive projectiles in a vacuum system to simulate damage to spacecraft structural materials [9–15]. The first approach is very expensive and time consuming. The velocity of the particles achieved by light gas guns is a maximum of 10 km s^{-1}. This is not suitable for comparing the data obtained in the long duration experimental profile where the upper velocity of the space debris particles is 40 km s^{-1}. An alternative approach is to use plasma drag accelerators to drive projectiles in a vacuum system to simulate minimum damage to the spacecraft structural material in space. An electromagnetic accelerator, capable of driving small projectiles to hypervelocity, was described by Rose *et al.* [9].

The operational sequence of the hypervelocity impact facility test set-up was as follows. Fig. 2 shows the block diagram of the electrical drives for accelerator capable of driving small projectiles of olivine particles to hypervelocity [9]. A capacitor bank connected eight capacitors, each 6.7 μF, in parallel) with a total capacitance of 53.6 μF, can be charged up to 50 kV ($E = 67$ kJ maximum) through a suitable resistor. Once the desired charging voltage is reached, a solid-state dielectric switch is triggered that results in a current pulse of 10^6–5×10^6 A flowing through an armature. The armature rapidly explodes producing an extremely hot plasma that expands through the launcher barrel. The details of materials, diagnostics, and controls of the entire hypervelocity impact test system are described elsewhere [9]. Particulates may be generated from the sources such as (a) the armature itself, (b) particles from the rails could be generated by ablation and recondensation, and (c) the ablator plate suitably loaded with the desired particles of different size. The third source provides the vast majority of the fragments in a controlled way. As the aluminium foil explodes, the hot plasma disintegrates a suitable plastic ablator plate into gases such as hydrogen and carbon at a temperature of several 1000 K. The plasma/gas, and desired particles are accelerated further down the drift tube through the skimmers (to collimate the debris particle stream). There will be many such projectiles travelling at substantial fractions of the plasma velocity; the plasma/debris cloud

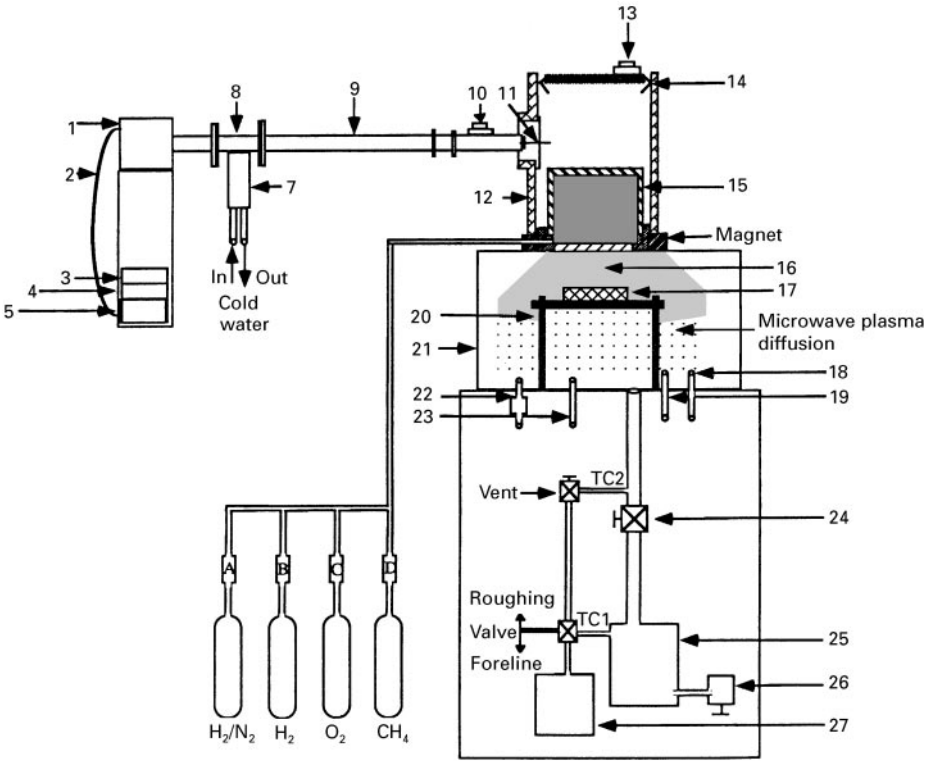

Figure 1 Schematic diagram of the microwave plasma disc reactor used to deposit diamond-like carbon in the down-stream mode. 1, Model S-1500 microwave power head; 2, power cable; 3, standard controller; 4, Model 247C, four channel readout; 5, model S-1500 microwave power supply; 6, (A, B, C, D) mass flow controllers; 7, dummy load; 8, circulator; 9, coxial waveguide; 10, plasma coupler side tuning stub; 11, adjustable power input probe; 12, brass housing (cavity wall); 13, plasma coupler top tuning stub; 14, sliding short; 15, quartz bell jar reactor, with "O" ring; 16, downstream microwave, plasma zone; 17, substrate; 18, type J thermocouple; 19, electrical feedthough; 20, aluminium tripod; 21, glass bell jar; 22, Baraton pressure transducer; 23, cold cathode gauge; 24, hi-vac value; 25, turbo pump; 26, turbo purge; 27, mechanical pump; TC1 and TC2 thermocouple gauges.

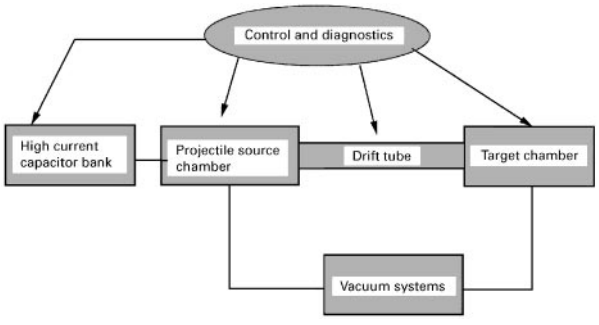

Figure 2 Block diagram of the hypervelocity impact test facility that consists of a capacitor bank, projectile source, drift tube, and a target chamber.

velocity, x, y co-ordinates, the number of impacting particles, the duration of optical flash, and approximate cone angle of ejecta, some of which have been measured by high-speed photography (Hadland Photonics IMACON-790 image converter camera utilized in the streak mode).

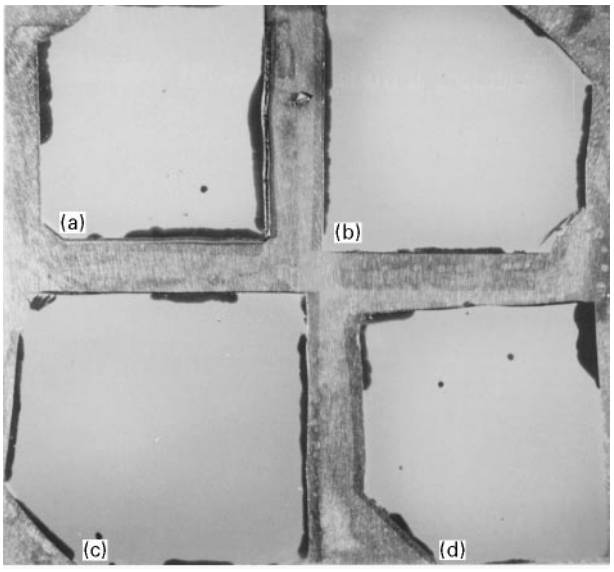

Figure 3 (a–d) Optical photographs of the polycrystalline diamond deposited over silicon substrates (4 numbers, each approximately 1 in^2, $\sim 6.45\ cm^2$) before the hypervelocity impact test.

3. Results and discussion

Fig. 3a–d show optical micrographs of the as-deposited polycrystalline diamond films grown over silicon substrates under identical conditions by microwave plasma technique using hydrogen and methane gas reaction mixture. Four diamond-coated silicon substrates were mounted over an aluminium supporting plate. We do not have the capability to grow diamond over 4 $in.^2$ ($\sim 25.8\ cm^2$) substrates in a single experimental run of microwave plasma deposition system; we could only grow on 1 $in.^2$ ($\sim 6.45\ cm^2$) substrate in an ASTeXs microwave plasma system. Therefore,

diamond was grown on four samples and mounted together to perform the hypervelocity impact test. The black spots on the samples of Fig. 1a, c and d are due to the wax that was formed during the mounting of the samples.

Fig. 4a–d shows optical micrographs of the polycrystalline diamond films subjected to hypervelocity impact tests. These tests were performed using 100 μm (145 grid) olivine particles [$(Mg, Fe)_2 SiO_4$]. Olivine is a mineral that contains iron and magnesium. This material is generally found in ultramafic rocks. Mafic is a word that defines igneous rocks with high iron and magnesium. Molten lava contains crystallized grains of olivine. The gem variety of olivine is called peridot. The meteorites contain mainly olivine in the low Earth orbit altitude zones. Fig. 5 is the magnified view of Fig. 4b where a large number of impact sites including the microcracks may clearly be seen with the naked eye. The colour in the crater area is different from the clean area. This may be due to the lifting or buckling of the film on the silicon substrate. The diamond film lifts in circular shapes.

Fig. 6a and b are scanning electron micrographs of an observed crater in a diamond film upon hypervelocity impact testing. Fig. 6b is a magnified view of Fig. 6a. It may be noticed from the micrographs that there are about nine cracks around the crater and which propagate away from the crater centre. We do not know a particular reason to estimate the number of cracks that should result upon hypervelocity impact. The diamond film is polycrystalline and in such a case it is difficult to predict the number of cracks. If it were a single crystal it may be possible to predict it to some extent using the diamond or substrate crystal structure. For example, in the case of silicon, natural cleavage of (1 0 0) silicon wafer will produce four pieces,

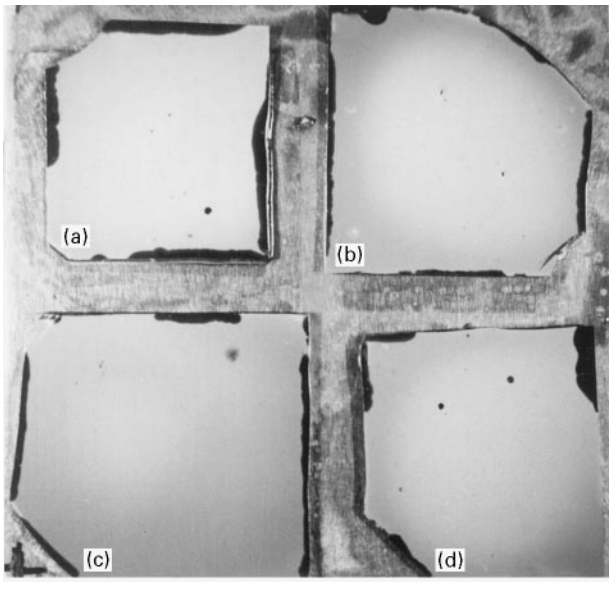

Figure 4 (a–d) Optical photographs of the polycrystalline diamond deposited over silicon substrates (4 numbers, each approximately 1 in^2, ~6.45 cm^2) after the hypervelocity impact test. Typical crater structures formed by 100 μm (145 grid) olivine particles [$(Mg, Fe)_2SiO_4$] impacting on a polycrystalline diamond-coated silicon (scratched) substrate by the hypervelocity impact tests. Olivine load = 30 mg.

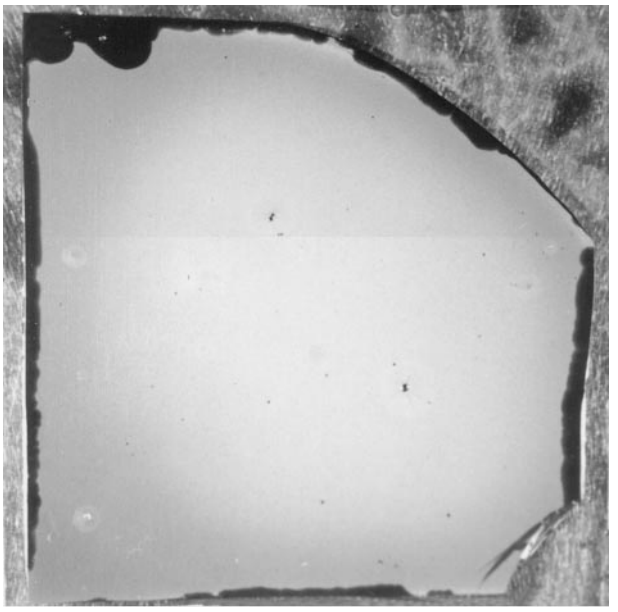

Figure 5 Magnified view of Fig. 4b showing the large number of impact sites observed on a diamond-coated silicon substrate after the hypervelocity impact test.

natural cleavage of (1 1 1) silicon wafer will give six pieces, and natural cleavage of (1 1 0) silicon wafer will give either four or seven pieces upon natural shocking. Gilath *et al.* [11] reported the fracture modes in alumina for plane and spherical shock waves for hypervelocity impact conditions. The crack propagates approximately to a length of 1 cm from the crater. These cracks may have been propagated from the base silicon substrate. However, we can offer no explanation to support this observation. It is technically disastrous if the diamond coating is used for space applications where hypervelocity impact by micrometeorites of a similar size to the olivine particles occurs. The diameter of the crater shown in Fig. 6a is approximately equal to 484 μm. The average crack width at the beginning of the crack is approximately 5 μm as per the electron micrograph shown in Fig. 6c. The crack width is approximately 3 μm at the halfway point of the crack shown in the electron micrograph of Fig. 6d. Typical morphology of a diamond film prepared by the microwave plasma may be seen in Fig. 6d. The morphology is very good. Raman analysis of as-deposited films on all the substrates was performed using a Renishaw 2000 Ramascope using a HeNe (633 nm, red) laser. All the films were confirmed to be diamond which also contains some non-diamond carbon inclusions.

Fig. 7a shows a scanning electron micrograph of another crater structure that was observed as a result of the hypervelocity impact test. We have observed nine microcracks in this crater structure also. Fig. 7b shows a magnified view of Fig. 7a. The diamond film has curled upwards as a result of impact in the impact zone (Figs 6 and 7). The centre of the crater is not circular as is observed in Fig. 6. The mechanism of crater formation and the type of shock wave may be different. The impact angle made with the surface of the diamond by the particle may be different. The nature of the diamond film in that region of the film

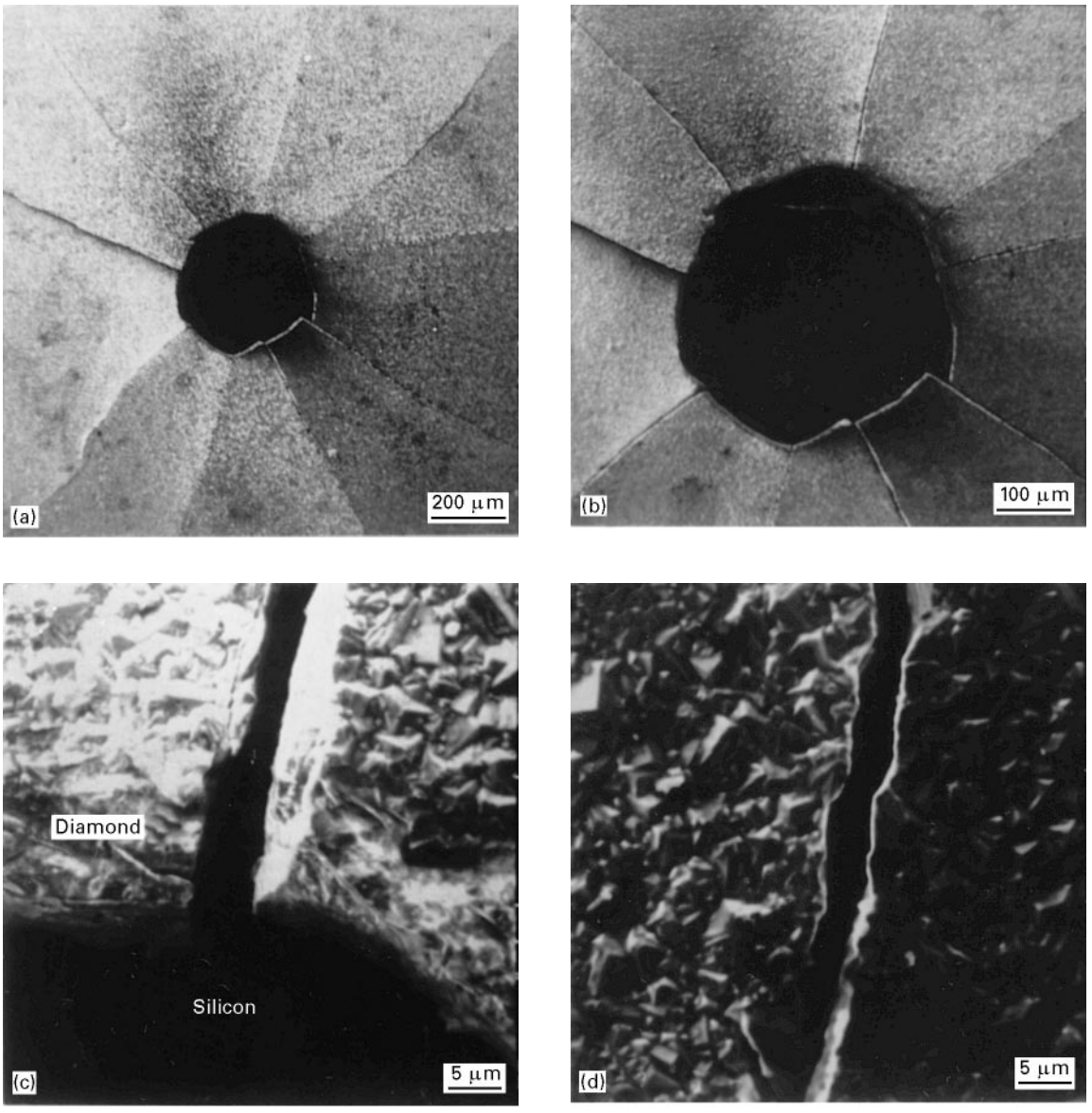

Figure 6 Scanning electron micrographs of an impact crater observed in the diamond thin films grown over the silicon substrate after hypervelocity impact test: (a, b) crater morphology, (c) initial dimensions of the crack, and (d) dimensions of the crack approximately at the centre.

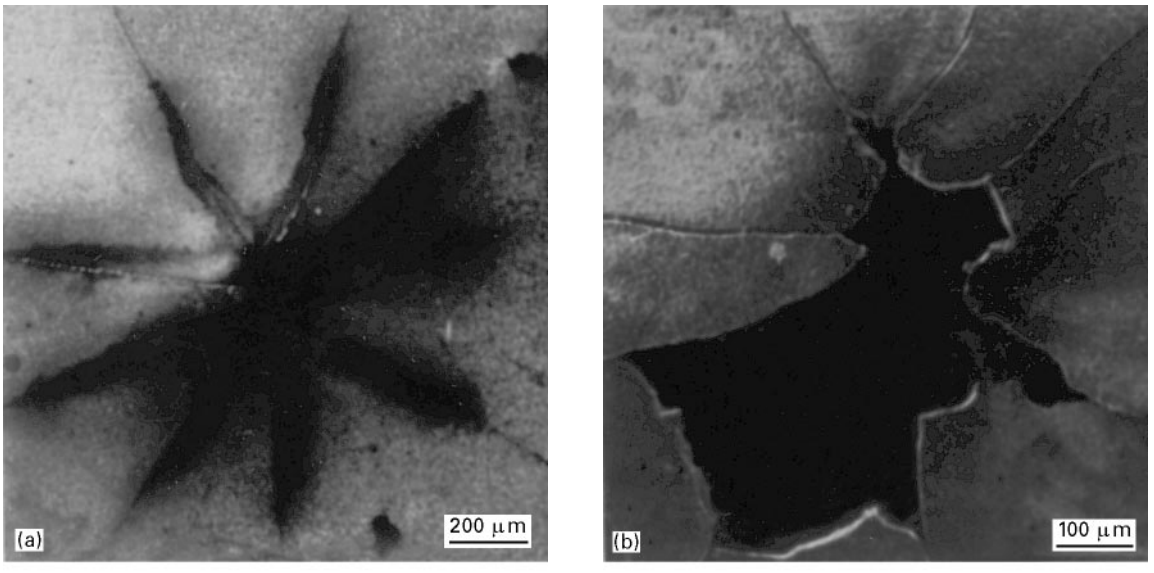

Figure 7 (a, b) Scanning electron micrographs of an impact crater observed after hypervelocity impact test showing crater morphology.

will also influence crater formation. The diamond film morphology varies from the centre of the substrate to the end of the surface, and this has been attributed to the variation in the substrate temperature during growth.

Fig. 8 show electron micrographs of the various craters observed over the diamond thin films. Fig. 8a and b are similar kinds of impact crater. Fig. 8c is a crater where the particle has penetrated into the

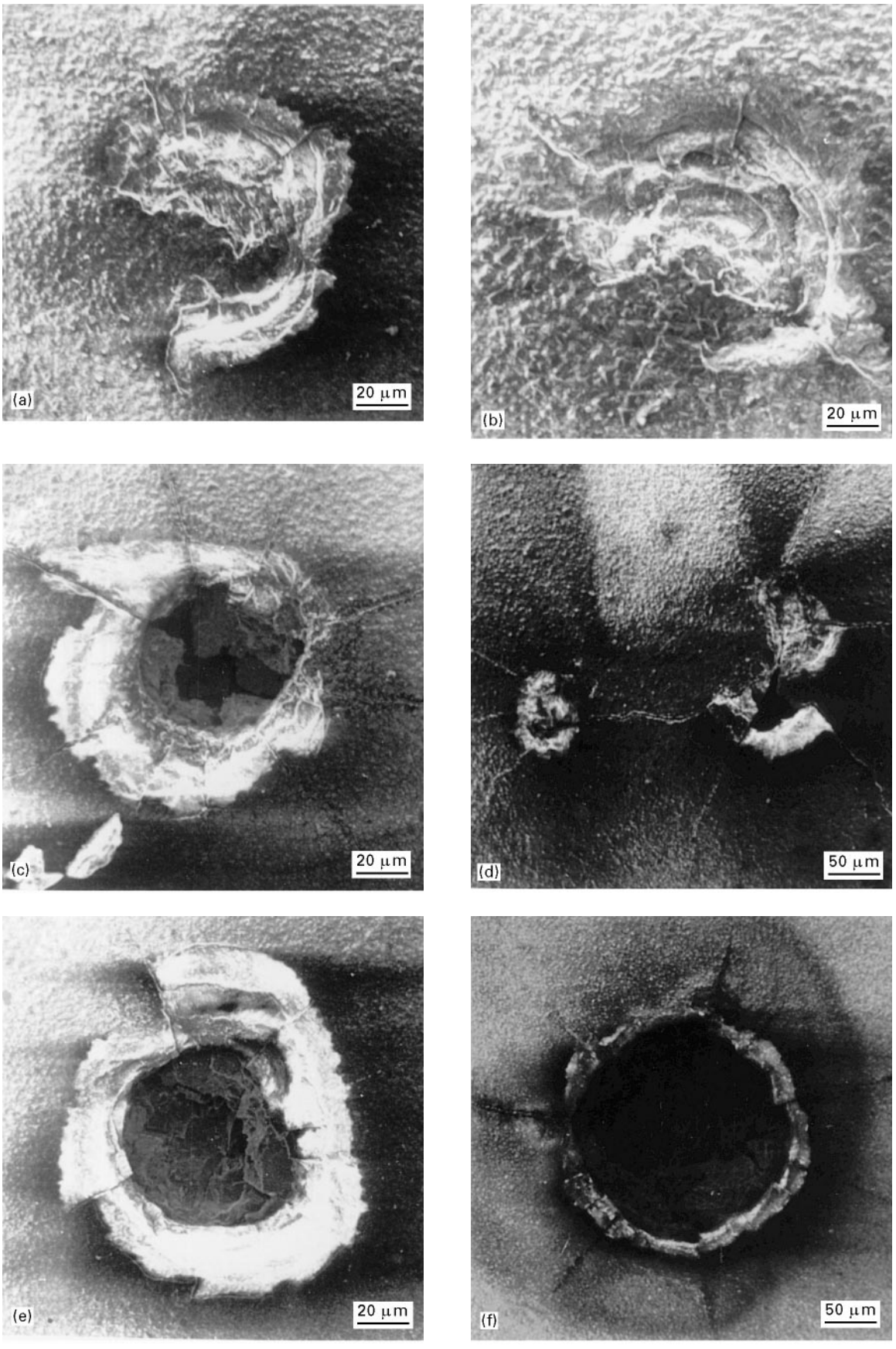

Figure 8 (a–f) Scanning electron micrographs of impact craters observed in the diamond thin film grown over the silicon substrate after the hypervelocity impact test, showing crater morphology.

silicon substrate. Fig. 8d shows the two impact sites formed by two different particles of different velocity. Fig. 8e and f are similar in kind; the crater structures are circular. Figure 8f has at least eight cracks visible to the naked eye. Several microcracks can be observed in the silicon wafer, some have propagated into the diamond thin films. These may be seen clearly in Fig. 8f.

Fig. 9 shows the streak camera photographs of the impact particles. Fig. 9a and b are negative and positive pictures of the impact particles, respectively. The negative picture has been shown because the nature of some of the crater particles can easily be identified. It is relatively easy to identify various particles using negative streak camera photographs and it is only our experience in the laboratory. No particles can be seen in the bright area of Fig. 9b whereas they are clearly visible in Fig. 9a. Some of the various characteristics of possible impact particles have been determined using streak camera photographs, such as the x, y coordinates of each impact, the number of impact particles, the velocity of each particle, the duration of the optical flash, the approximate cone angle of the ejecta, time of arrival, impact location, and velocity over the target plate. The velocity of the particle has been determined as follows: $V = D/T$, where D is the distance between gun and target. This was fixed at 710 cm in our experiments (Fig. 2). The streak camera was set at a streak rate of 25 $\mu s\,mm^{-1}$. Each particle will arrive at the target at a different time interval because each has a different velocity. Each bright spot in Fig. 9b or dark spot in Fig. 9a corresponds to the velocity of different particles. Time may be calculated by using an ordinary ruler to determine the length (mm) from the left side of the photograph of Fig. 9 and multiplying this by the streak rate (25 $\mu s\,mm^{-1}$). Once the distance (710 cm) and time of arrival corresponding to a particular impact particle is known, the velocity of that particle can be determined. In this way, velocities can be ascertained by manually determining the distance in Fig. 9, and the data are given in Table I. The closer the bright dot is to the Y-axis, the higher is the velocity at which that particle was travelling in the drift tube. In addition, the duration of the optical image is a measure of the plasma lifetime at the impact site. More details may be found elsewhere [9]. A mylar sheet was mounted parallel to and approximately an inch ($\sim$2.54 cm) away from the diamond film. The size of the hole formed in the mylar polymer is approximately equal to the diameter of the impact particle that has hit the target plate.

Table I shows the quantitative data obtained during the hypervelocity impact performed over four diamond samples (area $\approx$4 in^2, $\sim$25.8 cm^2 Fig. 4). In total, seven craters were analysed in this test. The eighth crater gives the reference co-ordinates for the

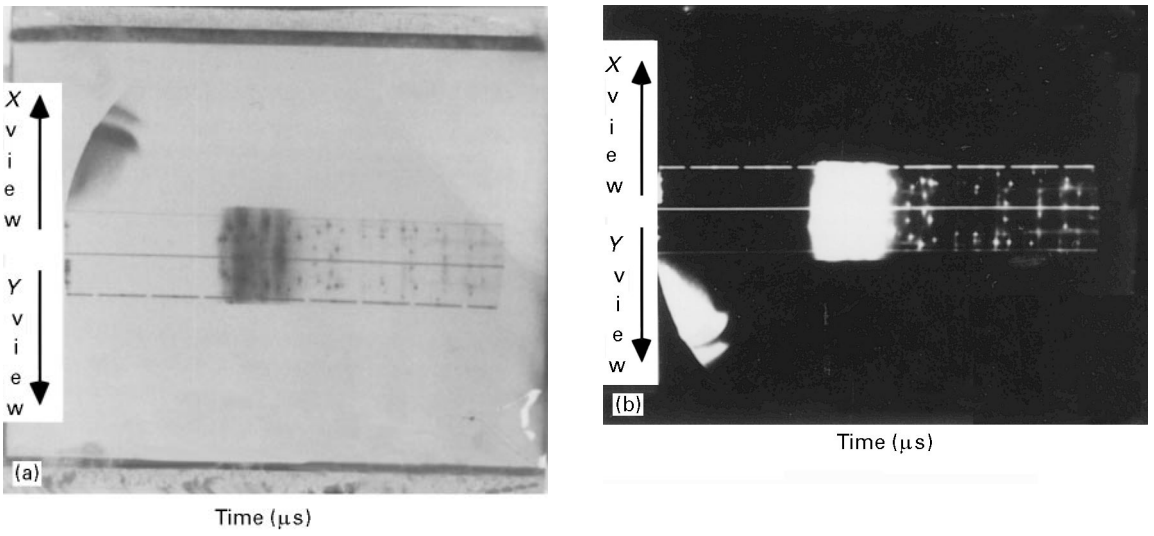

Figure 9 Streak camera photographs, (a) negative and (b) positive, after the hypervelocity impact test performed on the diamond-coated silicon substrate to evaluate particle arrival time, impact location, and velocity at the target plate.

TABLE I Hypervelocity impact test results on diamond/silicon (total area 4 in^2, $\sim$25.8 cm^2)

Crater	X (m)	Y (mm)	Impact size ($\mu m \times \mu m$)	Hole size in mylar ($\mu m \times \mu m$)	Spall/chip in diamond ($\mu m \times \mu m$)	Particle velocity ($km\,s^{-1}$)
1	34.1	31.5	190 × 150	20 × 25		8
2	41.8	59.3	55 × 30	40 × 70	105 × 75, 64 × 35	7.3
3	52.9	61.3	72 × 120, 300 × 200	71	2378 × 1175	5.5
4	42.25	44.5	310 × 350	105 × 55	780	4
5	11	18.6	149 × 73	25 × 45	–	3.7
6	48.2	58	200	35 × 60	1400	3.6
7	67.3	57.1	60	33 × 53	950	3.4
8	0	0	Origin	–	–	–

sample set-up. X and Y are the co-ordinates of seven craters with respect to the reference crater (left corner of Fig. 4). The impact crater diameter varies from 60 μm to 310 μm. The approximate dimensions of the impact crater are given in Table I. Mylar film that was mounted 1 in. (2.54 cm) away from the target was used to determine the size of the impact particles: the maximum size observed was 105 μm, when olivine particles of 100 μm were used. This indicates that the hole dimensions measured in mylar film correlate with the particle size employed. The hole dimensions corresponding to the various debris particles are also presented in Table I. The maximum spall/chip size was found to be 2378 μm. Although the particle size used was 100 μm, the spall/chip size was significantly higher. The kinetic energy of the particle was converted into shock waves which spalled or chipped the diamond film in to particles of larger dimensions. This has a catastrophic effect on the diamond coatings. The velocities of the debris particles are also listed in Table I; that observed in this test was 8 $km\,s^{-1}$. Several microcracks were observed around the craters, and the film was buckled at some of the impact sites.

Although the olivine particle size used was 100 μm for hypervelocity impact tests, the observed crater size was completely different, as shown in Table I. The maximum velocity of the bombarded particles may be in the range 3.4–8 $km\,s^{-1}$. The olivine particles with this velocity truly penetrate 10–30 μm thick the diamond coating material. The craters on the substrate could be visually observed. Although the diamond is the hardest material known, in the literature thinner coatings of diamond are reported to not withstand the hypervelocity impact test with olivine particles. We feel that the diamond films may not withstand the hypervelocity impact test, irrespective of the type of impact particles chosen for the study. Experiments in our laboratory suggest that the thinner diamond coatings may not be applicable for protective coating applications in space because the particles truly penetrate the diamond thin film and the silicon substrate. Coatings for application space components should be thick enough to withstand the micrometeoroid particle impact and at the same time should have very good adhesive strength to the space components. Therefore, the survivability of the coating will be significantly high. The growth temperature for diamond is 800–1000 °C. Most of the materials have a higher thermal expansion coefficient when compared with diamond; therefore, adhesion of thick diamond to the substrate will be poor.

Fig. 10 shows an optical micrograph of the diamond-like carbon coated on the 3 in. (~7.62 cm) diameter silicon substrate. A shadow mask was used to measure the thickness of the film. The light triangular area is a masked area and was used to measure the thickness after the growth using a Tencor profilometer. It was possible to deposit the carbon over a 3 in. diameter silicon substrate directly at room temperature using a microwave plasma disc reactor. One wafer was subjected to a hypervelocity impact test: over 200 craters were observed in this test. The characteristics of some of the craters were analysed. Fig. 11 shows optical micrographs of typical crater

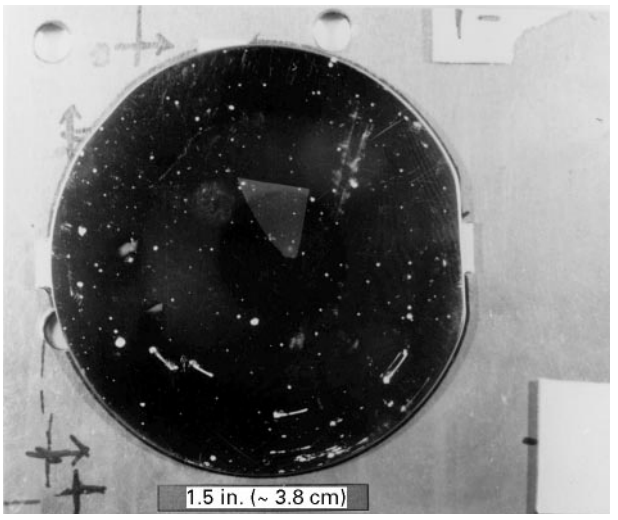

Figure 10 Magnified optical photograph of a large number of impact sites (over 200 craters) observed on a diamond-like carbon-coated silicon substrate (3 in, ~ 7.62 cm, diameter) after the hypervelocity impact test. Typical crater structures are formed by 100 μm (145 grid) olivine particles [$(Mg, Fe)_2SiO_4$] impacting on a polycrystalline diamond-coated silicon (scratched) substrate by the hypervelocity impact tests. Olivine load = 30 mg.

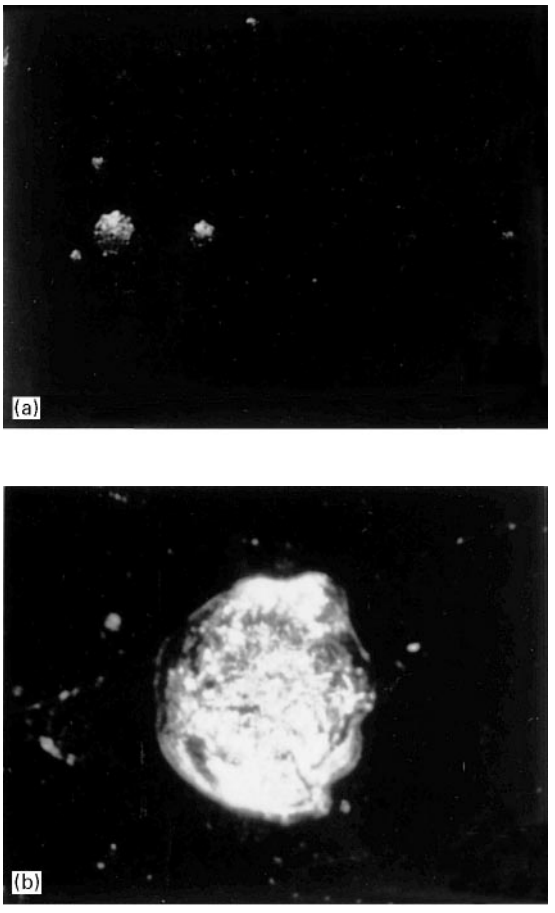

Figure 11 (a, b) Optical micrographs of the craters formed in the diamond-like carbon films shown in Fig. 10.

structures observed in diamond-like carbon thin films. However, we have no data from the electron micrographs of the crater structures observed in diamond-like carbon thin films.

Fig. 12 shows the streak camera photographs of the impact particles during the test performed over the

diamond-like carbon thin films. Various characteristics of the impact particles were determined using streak camera photographs such as time of arrival, impact location, and velocity over the target plate. The velocity of the particle was determined using the distance between the gun and the target plate (710 cm) and the time of arrival for that particular impact particle. The streak camera was set at a streak rate of 25 $\mu s\,mm^{-1}$. Various characteristics that have been obtained during the impact test on diamond-like carbon thin films are summarized in Table II. The velocity range observed in this test was in the range 4.2–7.8 $km\,s^{-1}$. The dimensions of the holes formed in the mylar film were the range 50–178 μm, whereas the diameter of the impact site in the diamond-like carbon films was in the range 350–1626 μm. This is significantly higher than the hole formed in the mylar film. Shock waves generated in the substrate upon hypervelocity particle might have caused this deleterious effect. Cracking has been observed in these micrographs but without the particular pattern that was observed in diamond films.

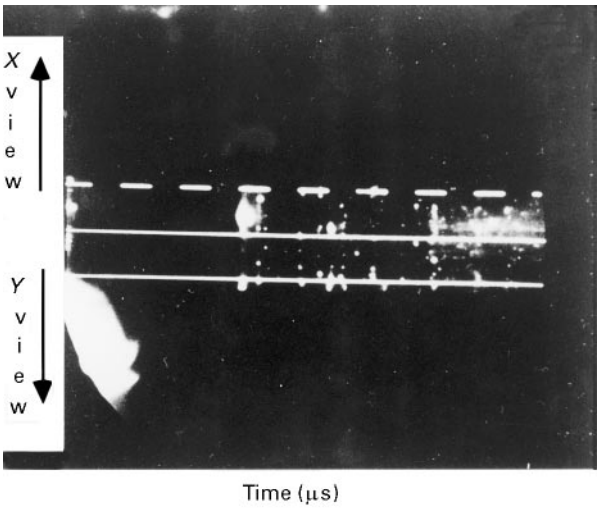

Figure 12 Streak camera photograph (positive) after the hypervelocity impact test performed on the diamond-like carbon-coated silicon substrate to evaluate particle arrival time, impact location, and velocity at the target plate.

4. Conclusion

Hypervelocity impact tests were performed on diamond and diamond-like carbon-coated silicon substrates using olivine particles. Thinner coatings could not withstand the impact tests performed with 100 μm olivine particles. These particles penetrated the diamond and diamond-like carbon film and the silicon substrate. The particle velocity obtained in these tests was approximately 8 $km\,s^{-1}$. Several microcracks were observed in the region of craters and these cracks propagated roughly a centimetre from the origin of the crack. The number of cracks observed was nine around the crater; the significance of this number is yet to be understood. Caution must be excercised in using diamond coatings for space components as protective coatings or as a window material [16, 17]. Diamond is transparent in the ultraviolet to far infrared region, and therefore it is a very good optical window material. Unfortunately, it may not withstand hypervelocity impacts in space. We have no data for thick diamond films (1 mm) at the present time. There is a problem in using polycrystalline diamond for optical window applications, due to the lack of surface smoothness and the required mechanical strength; this observation should not be overlooked in such optical window applications [18]. The studies performed in this paper on diamond and diamond-like carbon films reveal that they are very susceptible to damage by hypervelocity impact particles.

Acknowledgements

This work was carried out at the Space Power Institute of the Auburn University and was supported in part by the Naval Surface Warfare Center, Crane, IN, through Port Hueneme, CA, and by the Center for Commercial Development of Space Power (CCDS) and Advanced Electronics, located at Auburn University, with funds from NASA Grant NAGW-1192-CCDS-AD, Auburn University, Center's Industrial Partners, and in part by the Office of Innovative Science and Technology (SDIO/TNI) of the Strategic Defense Initiative Organization's Office through Navy Contract N60921-91-C-0078 with the Naval Surface Warfare Center. This work was partially supported by the National Science Foundation under Grant 9509842.

TABLE II Hypervelocity impact test results on diamond-like carbon/silicon (total substrate area ≈ 7 in^2)

Crater	Impact size (μm × μm)	Hole size in mylar (μm × μm)	Cracking in diamond (μm × μm)	Particle velocity ($km\,s^{-1}$)	Comments
A	432 × 395	32 × 42	587 × 509	7.8	Medium cracking
B	1626 × 1348	178 × 112	Negligible	4.4	Large; virtually no cracking
C_1	631 × 442	27 × 80	912	6	Upper impact; mutual cracking, double
C_2	541 × 512	80 × 70	912	6	Lower impact; mutual cracking, double
D	350 × 300	50	392	8	Medium cracking with small satellite craters
E	1309 × 927	85 × 125	Negligible	4.2	Large, virtually no cracking
	440 × 350	42 × 65	Negligible	4.2	Medium size, very little cracking
G	464 × 582	50 × 60	724	6.5	Medium size, very little cracking
H	213 × 273	32 × 40	529 × 492	6.5	Medium size, much cracking
I	760 × 850	140 × 60	None	5	Large, near edge, no cracking

References

1. J. E. FIELD, "The Properties of Diamond" (Academic Press, London, 1979).
2. J. H. EDGAR, *J. Mater. Res.* **7** (1992) 237.
3. H. C. TSAI and D. B. BOGY, *J. Vac. Sci. Technol* **A(5)** (1987) 3257.
4. J. W. GEHRING and R. L. WARNICA, in "Proceedings of the 6th Hypervelocity Impact Symposium, III, 2, (1963) p. 627.
5. H. A. SHAW, M. COLE, P. J. NEWMAN, M. E. SHAW, Y. TZENG, R. PHILLIPS, T. SRIVYNYUNON and A. JOSEPH, in "Proceedings of the Workshop on Hypervelocity Impacts in Space" (edited by J. A. M. McDonnell, unit for space sciences, University of Kent, Canterbury, UK, 1991) p. 62.
6. R. RAMESHAM, T. ROPPEL, C. ELLIS, D. A. JAWORSKE and W. BAUGH, *J. Mater. Res.* **6** (1991) 1278.
7. J. L. DAVIDSON, C. ELLIS and R. RAMESHAM, *J. Electron Mater.* **18** (1989) 711.
8. T. ROPPEL, D. K. REINHARD and J. ASMUSSEN, *J. Vac. Sci. Technol.* **B4** 1 (1986) 295.
9. M. F. ROSE, S. BEST and T. CHALOUPKA, in "Proceedings of 2nd Long-Duration Exposure Facility Post-Retrieval Symposium, (San diego, CA, 1992) NASA CP 3194, 1992, pp. 362–367.
10. R. RAMESHAM, D. C. HILL, S. R. BEST, M. F. ROSE, R. F. ASKEW and V. M. AYRES, *Thin Solid Films* **257** (1995) 68.
11. I. GILATH, S. ELIEZER and Y. GAZIT, *J. Mater. Sci.* **26** (1991) 2023.
12. R. LANGRATH, *Popular Science* **245** (1994) 32.
13. USAF Studies Hypervelocity Technology, *Aviation Week Space Technol.* **119** (1983) 62.
14. T. FOLGER, *Discover* **13** (1992) 14.
15. B. H. FORSTON and JAMES E. WINTER, *J. Test. Eval. Am. Soc. Test. Mater.* **21** (1993) 438.
16. W. P. SCHONBERG, *J. Spacecraft Rockets* **28** (1991) 118.
17. K. V. RAVI, *ibid.* **30** (1993) 79.
18. DANIEL C. HARRIS, "Infrared Window and Dome Materials", Vol. TT10 (SPIE Optical Engineering Press, Bellingham, WA, 1992).

Received 18 December 1995
and accepted 28 August 1996